example, to rotate independently around two different fivefold axes, at the same time slipping back and forth with respect to each other and to the metal, undergoing transitions from σ- to π-bonded states, bending some of the hydrogen atoms out of plane, and rearranging their C-C bond systems, while the metal changes its positions, at h_1 and h_2, with respect to each ring. It is not unreasonable to expect that a complicated conformational equilibrium involving significant population of the many simultaneous intermediate states of this process might produce a radial distribution which, if it could be calculated and refined, would reproduce the experimental radial distribution found by electron diffraction for the vapors of I without making use of the ABH conformation.

The dipole moment calculated for SS5 is rather large (4.7 D) compared to the experimental value (2.2-2.5 D). This could again be an artifact of the applied approximation or it may be related to the fact that SS5 is not really an optimized model. On the other hand, this discrepancy could also be the result of solvent effects, or the experimental value might be an average involving many different conformations including less polar ones such as, for example, the symmetrical (D_{5d}) sandwich.

As far as the IR investigations of beryllocene are concerned, it must be noted that the vibrational spectrum of one compound can often be interpreted to be consistent with many different models. The claim by Fritz and Sellmann[3] that, from the IR spectrum, a sandwich-type structure with asymmetrically placed Be atom is found in accordance with the result of the electron diffraction study is therefore probably somewhat unfounded in this specific and detailed formulation. The IR data are, therefore, probably not in real contrast to the present calculations.

Conformational analysis of molecules in the vapor phase is still a frontier of structural chemistry and very often our conclusions concerning the conformational behavior of undisturbed gaseous systems are uncertain. At present, hybrid theoretical and experimental techniques seem to offer the most powerful procedures in conformational studies of free molecules. The introduction of various expectation values into gas diffraction data analyses,[18,19,22] for example, has often made it possible to arrive at conclusions which could not have been obtained by applying individual techniques alone. The intimate connection and the complementarity of theory and experiment in studies of this kind seem to open a novel dimension in scientific research.

Acknowledgment. The authors wish to thank Dr. J. W. Wilkes for his support, the University of Arkansas Computing Center for executing the calculations, and Dr. N. S. Ostlund (Arkansas) and Dr. C. Giessner (Paris) for the use of their versions of Gaussian 70.

References and Notes

(1) A. Almenningen, O. Bastiansen, and A. Haaland, *J. Chem. Phys.*, **40**, 3434 (1964).
(2) A. Haaland, *Acta Chem. Scand.*, **22**, 3030 (1968).
(3) H. P. Fritz and D. Sellmann, *J. Organomet. Chem.*, **5**, 501 (1966).
(4) G. B. McVicker and G. L. Morgan, *Spectrochim. Acta, Part A*, **26**, 23 (1970).
(5) H. P. Fritz and R. Schneider, *Chem. Ber.*, **93**, 1171 (1960).
(6) M. Sundbom, *Acta Chem. Scand.*, **20**, 1608 (1966).
(7) O. Ya. Lopatko, N. M. Klimenko, and M. E. Dyatkina, *Zh. Strukt. Khim.*, **13**, 1128 (1972).
(8) C. H. Wong, T. Y. Lee, K. J. Chao, and S. Lee, *Acta Crystallogr., Sect. B*, **28**, 1662 (1972).
(9) C. Wong, T. Y. Lee, T. J. Lee, T. W. Chang, and C. S. Liu, *Inorg. Nucl. Chem. Lett.*, **9**, 667 (1973).
(10) C. H. Wong and S. M. Wang, *Inorg. Nucl. Chem. Lett.*, **11**, 677 (1975).
(11) E. O. Fischer and S. Schreiner, *Chem. Ber.*, **92**, 938 (1959).
(12) D. A. Drew and A. Haaland, *Acta Crystallogr., Sect. B*, **28**, 3671 (1972).
(13) D. S. Marynick, *J. Am. Chem. Soc.*, **99**, 1436 (1977).
(14) W. J. Hehre, R. F. Stewart, and J. A. Pople, *J. Chem. Phys.*, **51**, 2657 (1969).
(15) W. J. Hehre, W. A. Lathan, R. Ditchfield, M. D. Newton, and J. A. Pople, Program No. 236, Quantum Chemistry Program Exchange, Indiana University, Bloomington, Ind.
(16) W. J. Hehre, R. Ditchfield, R. F. Stewart, and J. A. Pople, *J. Chem. Phys.*, **52**, 2769 (1970).
(17) P. R. Bevington, "Data Reduction and Error Analysis for the Physical Sciences", McGraw-Hill, New York, N.Y., 1969.
(18) L. Schäfer, *Appl. Spectrosc.*, **30**, 123 (1976).
(19) M. Askarl, G. H. Paull, W. Schubert, and L. Schäfer, *J. Mol. Struct.*, **37**, 275 (1977).
(20) J. D. Dill, and P. v. R. Schleyer, and J. A. Pople, *J. Am. Chem. Soc.*, **98**, 1663 (1976).
(21) J. D. Dill and J. A. Pople, *J. Chem. Phys.*, **62**, 2921 (1975).
(22) W. K. Schubert, J. F. Southern, and L. Schäfer, *J. Mol. Struct.*, **16**, 403 (1973).

Extreme Conformational Flexibility of the Furanose Ring in DNA and RNA

Michael Levitt*[1] and Arieh Warshel

Contribution from the Laboratory of Molecular Biology, Cambridge, CB2 2QH, England.
Received May 31, 1977

Abstract: Consistent force field calculations have been used to calculate the variation of energy along the pseudorotational paths of ribose and deoxyribose rings. This energy changes by only 0.5 kcal/mol as the ring pucker changes from C3′-endo to C2′-endo. Therefore, the torsion angle ψ' of the sugar-phosphate backbone of nucleic acids is more flexible than a normal C-C single-bond torsion angle and cannot be frozen at a value corresponding to either of these puckers when other torsion angles are varied. An analytical expression for the variation of the ring energy and conformation as a function of ψ' is given to enable this extreme flexibility to be included in future calculations of nucleotide conformations. The finding that the furanose ring is so easily deformed has far-reaching implications about the structure of polynucleotides and the rigidity of DNA.

The furanose ring occupies a central position in the chemical structure of nucleic acids by linking phosphate groups into a backbone and providing attachment points for the bases. Any changes of conformation of this ring could have a profound effect on the possible conformation of DNA and RNA molecules. Previous calculations on nucleotide conformations[2-8] have chosen to keep the furanose ring fixed at one or two conformations but have allowed the single bond torsion angles in the backbone to vary continuously. Rigidly fixing the conformation of a five-membered ring would seem too limiting when one considers that cyclopentane can freely change the ring pucker along a path known as pseudorotation.[9-13] On the

0002-7863/78/1500-2607$01.00/0

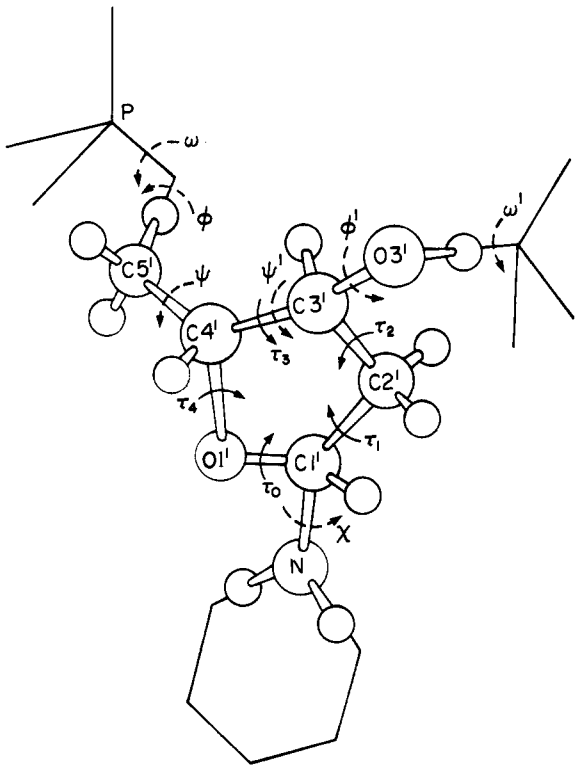

Figure 1. The deoxyribose form of the molecule studied and its relation to the phosphate backbone and base in polynucleotides. The small spheres represent the hydrogen atoms and the large spheres represent the heavier atoms (labeled with the atom names). The backbone torsion angle ψ' depends on the conformation of the ring with $\psi' \approx \tau_3 + 120°$. In the ribose form one hydrogen on C2′ is replaced by a hydroxyl group O2′-HO2′.

other hand, data from x-ray studies[11] do show that the furanose ring usually occurs close to one of two puckered conformations, C3′-endo or C2′-endo, depending on which of these two ring atoms is displaced out of the plane of the ring toward C5′. Another reason for fixing the ring conformation is that when the variables are single-bond torsion angles, a closed ring presents serious computational problems.

In this work the energetics of furanose ring puckering is analyzed completely by minimizing the molecular potential energy with respect to all the Cartesian coordinates. By constraining a selected variable and relaxing all other variables the energy variation has been mapped along the least energy path of distortion from the equipotential minima at the C3′-endo and C2′-endo puckering positions. The torsion angle ψ' passing through the ring is found to be the most flexible degree of freedom in the nucleic acid chain and cannot, therefore, be frozen at a C3′-endo or C2′-endo conformation.

I. Methods

The energy of the molecule studies here (Figure 1) is calculated by the consistent force field method using the standard QCFF/PI program.[14] In this procedure the potential energy is expressed as a sum of terms that describe bond stretching, bond angle bending, 1,3 Urey-Bradley interactions, bond twisting, van der Waals interactions, and charge-charge (electrostatic) interactions. The best values for the energy parameters have been found by fitting a large body of x-ray crystallographic, calorimetric, and spectroscopic data.[15,16] Here, the Urey-Bradley terms and $\theta\theta\phi$ coupling terms were omitted as they are needed mainly to reproduce spectroscopic data and do not affect conformation or energies. Because the molecule used here has polar groups that are not present in a nucleotide or nucleic acid (the NH_2 becomes the base, the O3′-HO3′ become part of the backbone), electrostatic interactions were initially eliminated by using a dielectric constant of ∞. Some calculations were, however, done with a dielectric constant of 1 and showed that the electrostatic energy could be calculated after minimization of an energy function that included all other terms. Although Figure 1 illustrates a deoxyribose ring, calculations were also performed on the ribose ring (an extra hydroxyl group O2′-HO2′).

An important feature of the present calculation is the complete relaxation of the conformation by changing all the atomic Cartesian coordinates until the energy was at a minimum value. A combination of steepest decent and Newton-Raphson iterations was used repeatedly until the energy remained constant to within 0.001 kcal mol^{-1} and the maximum forces were less than 0.0001 kcal mol^{-1} $Å^{-1}$. In this way stable conformations and their energies can be computed very accurately.

Energy minimization can also be used to find the lowest energy path between the different stable conformations. This is done by constraining one or more chosen variables to required values by means of an additional potential added to the molecular energy function. The new energy function is then minimized by changing all the Cartesian coordinates to give a conformation that satisfies the particular constraint yet is relaxed and has the lowest energy possible. The constrained variables are usually torsion angles, and by repeating the minimization for a range of constraint values, the energy can be mapped along any path in conformational space.

Here three different constraints are used. In the first, the backbone torsion angle ψ' passing through the ring (Figure 1), was constrained to values between 35 and 185° at 10° intervals. The artificial potential used was $1000\,(1 - \cos(\psi' - \psi'_0))$ kcal mol^{-1}, where ψ' is the current value of ψ' and ψ'_0 is the required value (i.e., from 35 to 185°). Because this constraint gives rise to very large forces when ψ' is not very close to ψ'_0 the energy contribution of this extra potential is always small and is subtracted from the molecular energy before plotting the energies.

The second constraint was introduced to force the five-membered furanose ring to follow the path of pseudorotation accurately. In pseudorotation, the ring changes its conformation so that the atoms move in and out of the mean plane without a large increase in energy. As the ring pucker changes, the ring torsion angles τ_j ($j = 0, 1, 2, 3, 4$) must also change in a cooperative way. Both τ_j and z_j, the out-of-plane displacement of ring atom C_j' ($j = 0$ for O1′), can be expressed as very simple analytical functions of an amplitude (τ_{max} or q) and a phase angle W (in degrees).

$$\tau_j = \tau_{max} \cos(W + j \times 144° - 288°)$$

$$z_j = (2/5)^{1/2} q \cos(W + j \times 144° - 90°)$$

The particularly simple expression for z_j follows from the particular way of choosing the mean plane through the five atoms. This plane, which is not a least-squares fit, is chosen to give $\Sigma_j z_j = 0 = \Sigma_j z_j \cos((j-1)72°) = \Sigma_j z_j \sin((j-1)72°)$. (An efficient way of finding this plane is given in ref 12.) z_j is positive for a displacement above the plane of the ring when the atoms are numbered in an anticlockwise sense (exo relative to C5′): when z_j is at a maximum positive value the ring is C_j'-exo; when z_j is at a maximum negative value the ring is C_j'-endo. τ_{j+2}, the torsion angle across the ring from atom C_j', is zero when C_j' is at one of these extreme values. Note that z_j is not a maximum when τ_j is at one of its extreme values. For a large number of furanose ring structures solved by x-ray crystallography[11] τ_{max} averaged to 39°. For cyclopentane an analysis of thermodynamic information (using the reduced mass along the pseudorotation coordinate)[10] gave $\tau_{max} = 44°$ and $q = 0.43$ Å.[21] This result was confirmed by electron diffraction measurements.[22] For the furanose ring our calculation

Table I. Ring Conformations, Torsion Angles, and Energy Contributions at the Ten Positions of Maximum Pucker

Ring conformation	Pseudorotation angle W, deg	Backbone angle ψ', deg	Energy,[a] kcal mol^{-1}			
			Total	Nonbond	Bond angle	Torsion
C3′-endo	18	82	−60.1	−69.4	3.46	5.86
C4′-exo	54	82	−60.0	−69.5	3.44	6.02
O1′-endo	90	96	−59.5	−69.3	3.49	6.30
C1′-exo	126	120	−59.7	−69.4	3.73	6.00
C2′-endo	162	144	−59.9	−69.4	3.45	6.01
C3′-exo	198	158	−59.0	−68.9	3.64	6.22
C4′-endo	234	158	−58.1	−69.0	2.73	8.17
O1′-endo	270	144	−57.7	−69.0	2.51	8.78
C1′-endo	306	120	−58.9	−69.8	2.92	7.96
C2′-exo	342	96	−59.5	−69.2	3.11	6.61

[a] The energy is estimated by interpolation from the energies calculated at 20° intervals of W.

gave $\tau_{max} = 43°$ at both the C2′-endo and C3′-endo conformations. The ring was forced to move on the pseudorotation path by a constraint energy given by

$$\sum_{j=0}^{5} 1000(1 - \cos(\tau_j - \tau_j{}^0)) \text{ kcal mol}^{-1}$$

where $\tau_j{}^0 = \tau_{max} \cos(W + j \times 144° - 288°)$ and τ_{max} was set to 40°.

The third constraint was used to define a less constrained path than pure pseudorotation: only τ_3 was constrained as $\psi' = \tau_3 + 120°$. Table I gives values of W, τ_3, and ψ' for the ten extremes of ring puckering.

II. Results

The variation of the energy of the ribose molecule with ψ' is shown in Figure 2. The steep rise in energy below $\psi' = 60°$ and above $\psi' = 170°$ is caused by bond angle bending as the ring puckering has reached its maximum extent. Between $\psi' = 80$ and 160° the ring pucker changes smoothly yet the energy passes over a small barrier of only 0.6 kcal mol^{-1}. Over this range of ψ', the C3′-C4′ bond is more flexible than if it had been a C-C single bond (upper dashed curve of Figure 2a).

For ψ' between 80 and 150°, the ring torsion angles change in the way expected for pseudorotation (Figure 2b). Between 150 and 180° they change more slowly than expected, and below 80° they remain constant as decreasing ψ' cannot have any further effect on the ring. Mapping the energy along ψ' cannot describe the complete path of pseudorotation as the ring has two conformations for each ψ' but the minimization method only finds the one of lowest energy.

The energy was, therefore, mapped by constraining the angle of pseudorotation W to values between 0 and 360°. When all the five ring torsion angles τ_j are constrained (by constraining W), the energy (Figure 3a, solid line) varies more than when only ψ' was constrained; the barrier between the C3′-endo pucker at $W = 18°$ and the C2′-endo pucker at $W = 162°$ is 1.4 kcal mol^{-1} instead of 0.6 kcal mol^{-1}. When only τ_3 is constrained to follow the pseudorotational path, the ring is able to relax more and have a lower energy (Figure 3a, dashed curve) at all values of W. The barrier between C3′-endo and C2′-endo is now 0.6 kcal mol^{-1} as found when only ψ' was constrained. The values of W observed experimentally cluster around the low-energy regions of the curve, although a few structures do have energies up to 2 kcal mol^{-1} above the minimum values.

When all the five τ_j are constrained according to eq 1 (with $\tau_{max} = 40°$) their variation with W is given by the smooth curves in Figure 3b. When only τ_3 is constrained the ring relaxes and the other four ring torsion angles no longer always fall on these curves (see symbols in Figure 3b). The deviations from pseudorotation are greatest when the energy along the path of pseudorotation is highest (between $W = 220$ and 320°).

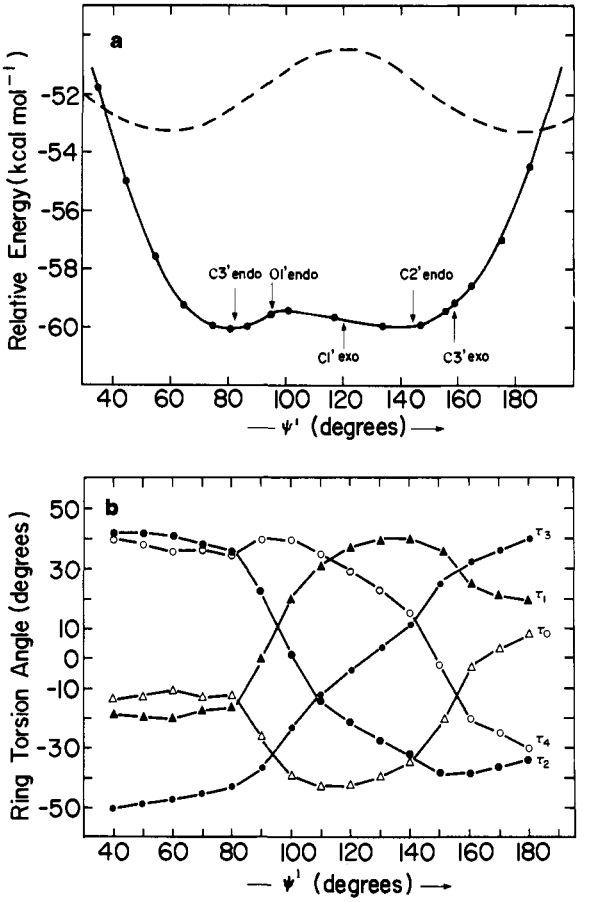

Figure 2. The variation of (a) the total energy and (b) the ring torsion angles as ψ' is constrained to values between 35 and 185°. This variation represents the way the ring changes as the backbone conformation changes. The absolute value of the energy is arbitrary; the dashed curve shows the energy variation expected for a C-C single bond.

These deviations from pseudorotation can be represented most clearly by showing both the angle of pseudorotation W and the puckering amplitude q (Figure 4). In pseudorotation q is constant as W changes from 0 to 360° so that the path of allowed ring conformations is a circle in the polar coordinate (q, W) plot. When all five τ_j torsion angles are constrained the conformations indicated as filled circles remain close to this circle, although the puckering amplitude is a little less than 0.4 Å for $70° < W < 120°$ and $240° < W < 300°$. When only τ_3 is constrained (open circles) the deviations are much greater: the ring becomes more planar for $240° < W < 300°$ as q decreases from 0.4 to 0.2 Å.

After obtaining the energy of the completely planar ring it was possible to express the ring energy as a simple analytical

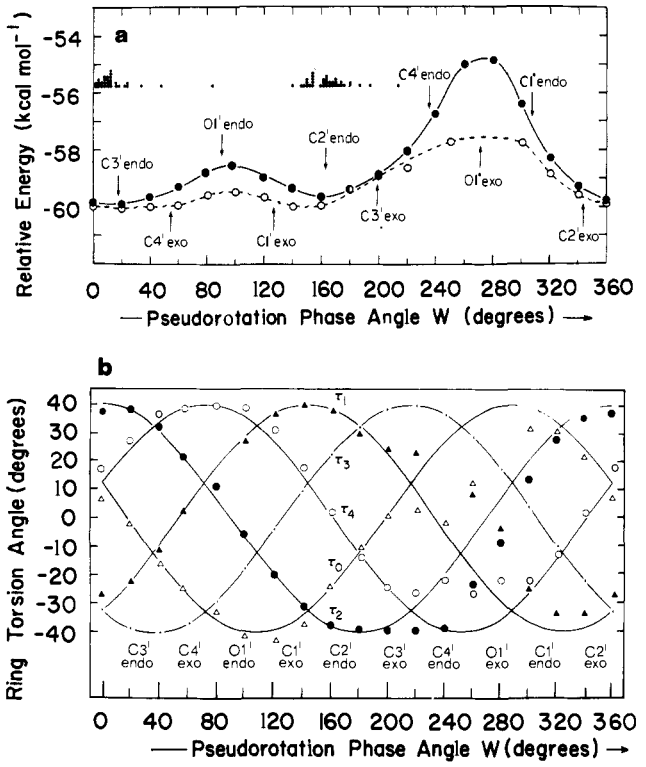

Figure 3. The variation of (a) the total energy and (b) ring torsion angles as the angle of pseudorotation W is constrained to values between 0 and 360°. This solid line shows the energy variation when all five τ_j are constrained to the path of pseudorotation and have values on the curves in (b). The dashed line shows the energy variation when only τ_3 is constrained to the path of pseudorotation. In this case the other four ring torsion angles move off the path and the energy is reduced. The dot histograms (a) mark the angles of pseudorotation observed in furanose structures solved by x-ray crystallography.[11]

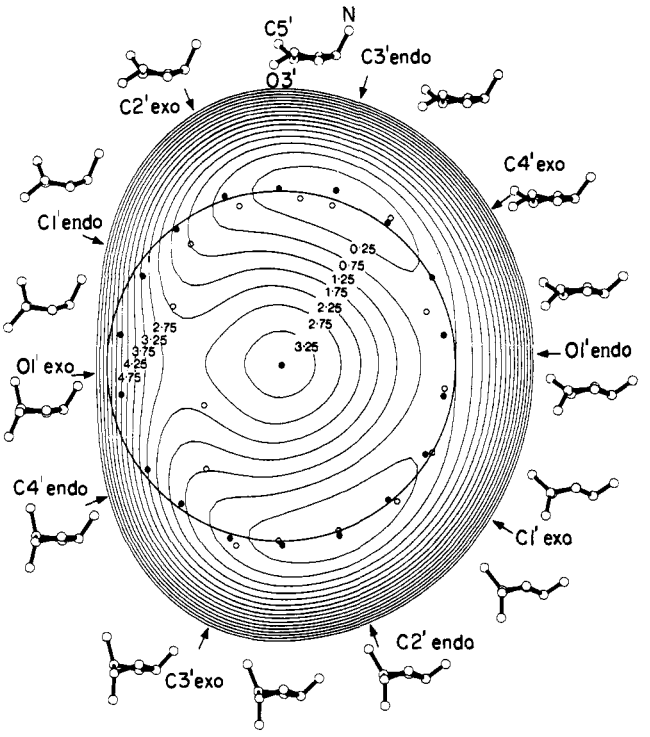

Figure 4. A complete energy map (kcal mol^{-1}) of the ring conformations in polar coordinates with W, the angular coordinate, increasing in a clockwise sense from a vertical value of $W = 0°$, and q, the puckering amplitude, increasing radially from the central dot (a completely planar ring). The ring is the path of true pseudorotation and has a radius corresponding to $q = 0.4$ Å. The filled circles mark conformations obtained when all five τ_j torsion angles were constrained to the path of pseudorotation (and also that of the completely planar ring). The empty circles mark conformations obtained when only τ_3 was constrained and all other variables allowed to relax. The conformations drawn are the relaxed conformations at the nearest empty circle on the energy map. The ring is viewed so that the mean plane is horizontal and endo displacements are up. The C4′-C3′ bond is approximately along the line of sight, with O3′ toward the viewer and C5′ away, so that the change in the backbone angle ψ' is clear. The ring atom O1′ is away from the viewer. Figure 3b shows the energy variation as a function of W only, i.e., taken around the ring path of pseudorotation.

function of q and W: $E(q, W) = a + b(W)q^2 + c(W)q^3$, where $a = 3.5$ kcal mol^{-1} is the energy of the planar ring (at $q = 0$) relative to the lowest energy (taken as zero). The functions $b(W)$ and $c(W)$ depend on the position and depth of the energy minimum as q varies for fixed W. If the minimum energy is β kcal/mol^{-1} at $q = \alpha$ Å, $b(W) = -3(\alpha - \beta)/\alpha^2$, and $c(W) = 2(\alpha - \beta)/\alpha^3$. The functional dependence of α and β on W was taken as $\beta = 0.8 - 0.9 \sin W - 0.8 \cos 2W$, $\alpha = 0.39 + 0.03 \cos 2W$ if $0° < W < 180°$, and $\alpha = 0.33 + 0.09 \cos 2W$ if $180° < W < 360°$, using the energies, q and W values of the conformations obtained by constraining τ_3. This energy function gives the approximate energy for any ring conformation. The energy contour map is symmetric about the horizontal line at $W = 90$ and 270°. At these two angles of pseudorotation, the ring oxygen atom O1′ is most out of plane at the endo and exo conformations, respectively. The symmetry of the contours about $W = 90°$ reflects the dyad (C_2) symmetry of the ring about a line through O1′ and bisecting the C2′-C3′ bond. Because the ring oxygen favors an open bond angle (>109°) more strongly than does the ring carbon atom, the energy is high when O1′ is maximally puckered ($W = 90, 270°$) and is low when O1′ is most in the plane (near $W = 0, 180°$). Calculations on oxolane,[13] the ring without the side groups, give an energy contour map that has minima at $W = 0$ and 180° and is symmetric about the lines $W = 0°$ and $W = 90°$. Here the symmetry about $W = 0°$ is broken by the side-groups interactions: the energy of O1′-exo is much higher than that of O1′-endo as the side groups C5′ and N approach each other too closely (see Figure 4).

In the above calculations the same relative energies (to within 0.1 kcal/mol^{-1}) were obtained for both deoxyribose and ribose rings. This is not surprising as electrostatic interactions were omitted from the energy function minimized. Early calculations showed that including charge-charge interactions with a dielectric constant of 1 changed the energies slightly but did not affect the minimum energy geometries (this is to be expected as electrostatic forces vary slowly with atomic position). Rather than repeat all the calculations with electrostatic terms, this extra energy was calculated at the conformations obtained above. The energy was found to depend on the orientation of the dipoles moments of the O3′-HO3′ and NH_2 groups. As both these groups are absent in polynucleotides, the dipoles moments were set to zero. For the deoxyribose group, the resulting variation of electrostatic energy (Figure 5) with pseudorotation angle W (only τ_3 was constrained) is only 0.05 kcal mol^{-1} from the mean value of −0.4 kcal mol^{-1}. For the ribose group the energy varies more but it is clear that the electrostatic term can have little effect on the total energy of the ring.

III. A "Black Box" Ribose

In energy calculations on nucleotides, the usual variables are the single bond torsion angles ϕ, ϕ', ω, ω', ψ, and χ (see Figure 1). ψ' is not varied but instead fixed at a value near 80° for the C3′-endo pucker and near 140° for the C2′-endo pucker. The above results show that the energy changes by only 0.6 kcal mol^{-1} as ψ' moves between 75 and 155° so that ψ' must be allowed to vary in the same way as the other torsion angles.

Table II. Cartesian Coordinates and Some Torsion Angles of Ten Relaxed Conformations[a]

Atom and coordinate	Nominal pseudorotation phase W (in degrees)									
	0	20	40	60	80	100	120	140	160	180
C5′ x	−1.87	−1.94	−1.99	−1.98	−2.00	−2.02	−2.01	−1.94	−1.79	−1.59
y	−1.65	−1.68	−1.71	−1.71	−1.71	−1.65	−1.51	−1.33	−1.16	−1.05
z	−0.67	−0.53	−0.42	−0.48	−0.51	−0.66	−0.92	−1.22	−1.44	−1.60
H51 x	−1.53	−1.71	−1.91	−1.88	−2.04	−2.09	−2.00	−1.74	−1.41	−1.05
y	−1.57	−1.64	−1.67	−1.64	−1.59	−1.43	−1.17	−0.86	−0.62	−0.48
z	−1.75	−1.61	−1.52	−1.57	−1.60	−1.73	−1.94	−2.14	−2.25	−2.31
H52 x	−1.78	−1.84	−1.82	−1.81	−1.79	−1.80	−1.83	−1.80	−1.69	−1.49
y	−2.70	−2.72	−2.75	−2.75	−2.76	−2.71	−2.58	−2.40	−2.23	−2.12
z	−0.37	−0.19	−0.09	−0.17	−0.26	−0.50	−0.88	−1.30	−1.61	−1.83
H53 x	−2.92	−2.99	−3.01	−3.01	−2.99	−2.99	−3.01	−2.98	−2.86	−2.66
y	−1.35	−1.36	−1.42	−1.42	−1.46	−1.43	−1.33	−1.14	−0.93	−0.79
z	−0.52	−0.32	−0.13	−0.20	−0.19	−0.35	−0.70	−1.13	−1.49	−1.76
C4′ x	−1.00	−0.99	−0.96	−0.97	−0.92	−0.91	−0.94	−0.98	−1.01	−1.02
y	−0.77	−0.76	−0.78	−0.79	−0.81	−0.82	−0.81	−0.79	−0.77	−0.77
z	0.16	0.21	0.24	0.22	0.21	0.16	0.10	0.01	−0.07	−0.15
H4′ x	−1.34	−1.22	−1.05	−1.07	−0.88	−0.84	−0.94	−1.16	−1.39	−1.56
y	−0.88	−0.83	−0.84	−0.87	−0.97	−1.07	−1.17	−1.26	−1.32	−1.36
z	1.23	1.30	1.34	1.32	1.30	1.24	1.12	0.94	0.74	0.55
O1′ x	0.38	0.38	0.37	0.38	0.37	0.36	0.35	0.36	0.37	0.37
y	−1.11	−1.10	−1.09	−1.09	−1.06	−1.04	−1.03	−1.05	−1.08	−1.10
z	−0.03	−0.08	−0.15	−0.14	−0.21	−0.23	−0.21	−0.16	−0.08	0.01
C3′ x	−1.00	−1.00	−1.04	−1.05	−1.08	−1.07	−1.03	−0.98	−0.96	−0.97
y	0.70	0.68	0.66	0.67	0.66	0.67	0.69	0.71	0.71	0.70
z	−0.23	−0.25	−0.23	−0.22	−0.13	−0.04	0.05	0.14	0.20	0.23
H3′ x	−1.01	−1.03	−1.18	−1.21	−1.52	−1.72	−1.83	−1.85	−1.84	−1.84
y	0.83	0.77	0.73	0.76	0.80	0.90	1.03	1.15	1.22	1.25
z	−1.32	−1.35	−1.33	−1.30	−1.17	−0.99	−0.77	−0.53	−0.35	−0.25
O3′ x	−2.09	−2.09	−2.07	−2.06	−1.89	−1.61	−1.29	−1.04	−0.95	−0.99
y	1.39	1.40	1.37	1.37	1.30	1.25	1.18	1.07	0.95	0.84
z	0.47	0.39	0.44	0.51	0.77	1.05	1.30	1.48	1.59	1.65
HO3 x	−2.21	−2.21	−2.23	−2.22	−2.09	−1.78	−1.38	−1.05	−0.91	−0.95
y	2.37	2.38	2.35	2.34	2.28	2.22	2.14	2.01	1.87	1.74
z	0.34	0.22	0.27	0.35	0.69	1.07	1.45	1.75	1.95	2.08
C2′ x	0.34	0.34	0.35	0.35	0.36	0.35	0.34	0.34	0.34	0.35
y	1.17	1.18	1.20	1.21	1.21	1.19	1.15	1.14	1.15	1.17
z	0.21	0.20	0.14	0.13	0.00	−0.10	−0.18	−0.23	−0.24	−0.23
H21 x	0.26	0.28	0.35	0.38	0.53	0.62	0.67	0.69	0.70	0.70
y	1.36	1.40	1.54	1.56	1.82	1.98	2.05	2.08	2.09	2.10
z	1.30	1.29	1.20	1.18	0.92	0.63	0.39	0.26	0.23	0.29
H22 x	0.68	0.67	0.64	0.64	0.52	0.39	0.28	0.21	0.20	0.23
y	2.09	2.09	2.04	2.03	1.83	1.58	1.38	1.28	1.28	1.37
z	−0.32	−0.35	−0.51	−0.54	−0.87	−1.11	−1.26	−1.33	−1.34	−1.31
C1′ x	1.28	1.28	1.28	1.28	1.28	1.27	1.27	1.27	1.27	1.27
y	0.00	0.00	0.00	0.00	0.00	0.00	0.00	0.00	0.00	0.00
z	−0.11	−0.07	0.00	0.00	0.13	0.21	0.24	0.24	0.20	10.13
H1′ x	1.99	1.95	1.86	1.86	1.72	1.62	1.58	1.58	1.63	1.72
y	−0.12	−0.14	−0.15	−0.14	−0.12	−0.09	−0.04	0.00	0.05	0.07
z	0.67	0.76	0.94	0.94	1.18	1.30	1.35	1.34	1.29	1.19
N1 x	1.96	2.02	2.14	2.14	2.29	2.36	2.39	2.39	2.35	2.28
y	0.09	0.10	0.10	0.08	0.04	−0.01	−0.04	−0.08	−0.12	−0.16
z	−1.45	−1.36	−1.16	−1.17	−0.81	−0.57	−0.45	−0.46	−0.58	−0.79
HN1 x	2.85	2.90	3.03	3.06	3.17	3.25	3.31	3.34	3.33	3.30
y	0.07	0.72	0.71	0.65	0.65	0.56	0.46	0.34	0.24	0.14
z	−1.62	−1.47	−1.13	−1.12	−0.60	−0.23	−0.03	−0.01	−0.18	−0.49
HN2 x	1.60	1.69	1.90	1.86	2.17	2.28	2.31	2.27	2.17	2.01
y	−0.47	−0.44	−0.47	−0.43	−0.56	−0.59	−0.59	−0.58	−0.58	−0.58
z	−2.26	−2.21	−2.06	−2.07	−1.71	−1.47	−1.37	−1.41	−1.56	−1.77
Actual W	7.8	21.0	39.4	39.6	73.1	98.2	118.8	138.6	159.7	182.5
ψ'	86.9	82.6	89.2	89.4	89.6	100.6	116.8	134.3	146.9	155.6

[a] Only τ_3 was constrained to a value dependent on the nominal pseudorotation phase W. Each conformation is in a coordinate system that puts the mean ring plane in the (x,y) plane.[12] The puckering of a ring atom relative to a plane through the other four ring atoms is approximately twice the puckering relative to the mean plane used here (the z coordinate).

This can be done in two ways. (a) In those cases where the energy is mapped as a function of pairs of backbone torsion angles, one only needs several standard ring conformations corresponding to different ψ' values (Table II). (b) If the energy is varied continuously as in a minimization to find the stable conformations, one needs an analytical representation of the ribose energy and conformation.

As the path of easiest distortion of the ring is close to pseudorotation (except where the energy is unfavorable), the obvious variable is the angle of pseudorotation W. The ring torsion angles τ_j and ψ' all depend on W as follows: $\tau_j = 40° \cos(W + j \times 144 - 288)$, $\psi' = 120° + \tau_3$. In practice only ψ' and two ring torsion angles, say, τ_1 and τ_2, need be calculated from W and used to give the Cartesian coordinates, x, of the ring.

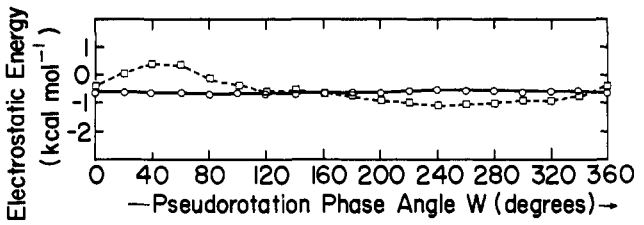

Figure 5. The variation of the electrostatic energy with angle of pseudorotation for ribose (dashed line) and deoxyribose (solid line) rings when only τ_3 is constrained to follow the path of pseudorotation. The conformations used were those obtained by minimization of the energy without electrostatic terms. A dielectric constant of 1 was used but the polar groups NH_2 and O3′-HO3′ were neutralized. For the ribose, the O2′-HO2′ bond was rotated to each of the three staggered positions but, as the energy was always lowest for the angle HO2′-O2′-C2′-C3′ = 60°, only this value is plotted. Note that in this staggered position, the O2′-HO2′ dipole is directed toward the negatively charged ring atom O1′. The partial charges in electronic units were as follows: C5′, −0.237; H5′, 0.079; C4′, 0.177; H4′, 0.079; O1′, −0.512; C2′, −0.158; H2′, 0.079; C1′, 0.177; H1′, 0.079; for ribose O2′, −0.267; HO2′, 0.267.

All bond lengths and angles are kept fixed and the internal energy of the whole ring system is also calculated from W as $E_{ring} = 0.8 - 0.9 \sin W - 0.8 \cos 2W$. The derivative of the total energy with respect to this new variable W is obtained from

$$\partial E/\partial W = -0.9 \cos W + 1.6 \sin 2W + (\partial E/\partial \psi')(\partial \psi'/\partial W) + (\partial E/\partial \tau_1)(\partial \tau_1/\partial W) + (\partial E/\partial \tau_2)(\partial \tau_2/\partial W)$$

where $\partial E/\partial \psi'$, $\partial E/\partial \tau_1$, and $\partial E/\partial \tau_2$ are evaluated from the Cartesian coordinate derivative $\partial E/\partial x_k$ using $\partial x_k/\partial \tau$, and $\partial \Psi'/\partial W$, $\partial \tau_1/\partial W$, and $\partial \tau_2/\partial W$ are evaluated from the analytical relationship between these angles and W. In this way, the minimization routine changes W, and the above relationships are used to give the changes in ψ', τ_1, and τ_2 that are then applied to the coordinates before calculating the energy. The derivatives of the energy with respect to ψ', τ_1, and τ_2 are then transformed to a derivative with respect to W for use by the minimization algorithm.

IV. Discussion

This work has shown that the furanose ring has two minimum energy conformations at the C3′-endo and C2′-endo ring puckerings and that the barrier between these minima is only 0.6 kcal mol^{-1}. This result has a simple physical explanation. First consider a five-membered ring of equivalent atoms like the cyclopentane ring. Because the ring closes on itself, the torsion angles about all five C–C single bonds must be close to the unfavorable eclipsed position at $\tau_j = 0°$. These unfavorable interactions make ring closure difficult, but once the ring is formed the energy is equally unfavorable for all the conformations along a path in conformational space known as pseudorotation. In the ring of the furanose system one methylene group is replaced by an oxygen. As the barrier to internal rotation is lower about a C–O single bond than about a C–C single bond (we have used barrier heights of 2.1 and 2.32 kcal mol^{-1}, respectively), the ring will prefer a conformation where the C–O torsion angles are most eclipsed. When these torsion angles, τ_0 and τ_4, are zero, the ring atoms across the ring from them, C3′ and C2′, will be maximally puckered and these two conformations (C3′-endo and C2′-endo) will be energy minima.

As the COC bond angle prefers a larger value than the CCC bond angle (we have used $E_{COC} = 40(\theta_{COC} - 2.09)^2$ kcal mol^{-1} and $E_{CCC} = E_{CC} = 30(\theta_{CCC} - 1.91)^2$ kcal mol^{-1} with the bond angles expressed in radians), the ring will have a high energy when the oxygen O1′ is maximally puckered (O1′-endo and O1′-exo). In the actual calculation the value of θ_{COC} varied from 108° when O1′ is most out of the mean plane to 115° when O1′ was most in that plane. The corresponding values for the four θ_{CCC} and θ_{CCO} angles were 102 and 105°, respectively. The height of the barrier between C3′-endo and C2′-endo depends sensitively on the difference between the energy parameters used for the ring carbon atoms and ring oxygen atom. This difference is probably overemphasized here (especially for bond angle bending) and the ring may even be more flexible. Cremer and Pople obtained barriers between 0.3 and 0.65 kcal mol^{-1} in ab initio calculations on oxolane,[13] the unsubstituted ring.

Although the energy of a furanose ring is found here to be almost constant between the C3′-endo and C2′-endo conformations, ring conformations observed by x-ray crystallography do tend to cluster at these two extremes (see Figure 3a). A possible explanation for this is the influence of crystal packing forces acting on the C5′ and O3′ atoms. As the energy of the ring system varies only slightly as ψ' changes from 80° (C3′-endo) to 150° (C2′-endo), but rises steeply outside these extremes (like an infinite box potential), any packing force that varies monotonically with ψ' in this range will force ψ' to one of these extremes[23]. The one crystal with an unusual O1′-endo pucker, dihydrothymidine, has ψ' near 100° and as there is rotational disorder about the C4′–C5′ bond, the packing constraints on the ring seem small.[17]

The variation of the energy of the ring system is almost the same for both the ribose and deoxyribose group: the extra hydroxyl group does not affect the conformational preferences of the ring. As ribonucleic acid double helices have only been observed in the C3′-endo conformation, while deoxyribonucleic acids double helices have been observed in both the C3′-endo and C2′-endo conformations,[18] this difference must be due to interactions of the O2′ hydroxyl group with the more distant parts of the sugar–phosphate backbone. Single-stranded ribonucleic acid does adopt both puckers.[11]

The finding that the furanose ring is so easily deformed has some important consequences. Firstly, all previous energy calculations[2-8] have kept the furanose ring at a fixed pucker (usually C3′-endo and C2′-endo) while varying the backbone torsion angles to find allowed conformations. This separation of variables is totally unjustified and flexibility of the furanose ring will have to be included to get any meaningful results. This is particularly true as changing the torsion angle ψ' over the range 70 to 160° has a considerable effect on the relative positioning of the base and backbone.

Secondly, the structures of polynucleic acids have been determined by fitting models to the rather limited fiber diffraction data.[18,19] In this procedure, the ribose conformation was fixed and the single bond torsion angles were varied to get the best fit to the x-ray data. Once again, because the ribose is actually more flexible than a C–C single bond (Figure 1), this separation of variables is wrong. When the sugar ring is represented with its proper flexibility, it may be possible to get a better fit to the x-ray data.

Thirdly, the variation of the furanose ring energy with ψ' is different from the energy variation of other single bonds that have a threefold potential: the energy is almost flat from $\psi' = 70°$ to $\psi = 160°$ and rises steeply outside this range. Thus, the furanose ring conformation is continuously variable in this region and not restricted to the same staggered positions as C–C single bond. In any smooth deformation of a polynucleic acid, the ribose can change smoothly to accommodate the necessary strains. Such smooth bending[24] would enable DNA to wind around the histone core in chromatin without any sharp kinks.[20]

References and Notes

(1) To whom correspondence should be addressed.
(2) V. Sasisekharan, A. V. Lakshminarayanan, and G. N. Ramachandran In

"Conformation of Biopolymers", Vol. 2, G. N. Ramochandran, Ed., Academic Press, New York, N.Y., 1967, p 641.
(3) V. Sasisekharan and A. V. Lakshminarayanan, *Biopolymers*, **8**, 505 (1969).
(4) W. K. Olson and P. J. Flory, *Biopolymers*, **11**, 1 (1972).
(5) S. B. Broyde, S. D. Stellman, and R. M. Wartell, *Biopolymers*, **14**, 2625 (1975).
(6) S. B. Broyde, R. M. Wartell, S. D. Stellman, B. Hingerty, and R. Langridge, *Biopolymers*, **14**, 1597 (1975).
(7) O. E. Millner, Jr., and J. A. Andersen, *Biopolymers*, **14**, 2159 (1975).
(8) V. E. Khutorsky and V. I. Polter, *Nature (London)*, **264**, 483 (1976).
(9) J. E. Kilpatrick, K. S. Pitzer, and R. Spitzer, *J. Am. Chem. Soc.*, **69**, 2483 (1947).
(10) S. Lifson and A. Warshel, *J. Chem. Phys.*, **49**, 5116 (1968).
(11) C. Altona and M. Sundaralingam, *J. Am. Chem. Soc.*, **94**, 8205 (1972).
(12) D. Cremer and J. A. Pople, *J. Am. Chem. Soc.*, **97**, 1354 (1975).
(13) D. Cremer and J. A. Pople, *J. Am. Chem. Soc.*, **97**, 1358 (1975).
(14) A. Warshel and M. Levitt, Quantum Chemistry Program Exchange, No. 247, Indiana University, 1974.
(15) A. Warshel and S. Lifson, *J. Chem. Phys.*, **53**, 582 (1970).
(16) (a) A. Warshel and M. Karplus, *J. Am. Chem. Soc.*, **94**, 5613 (1972); (b) A. Warshel in "Modern Theoretical Chemistry", Vol. 7, G. Segal, Ed., Plenum Press, New York, N.Y., 1977.
(17) J. Konnert, I. L. Karle, and J. Karle, *Acta Crystallogr., Sect. B*, **26**, 770 (1970).
(18) S. Arnott, S. D. Dover, and A. J. Wonacott, *Acta Crystallogr., Sect. B*, **25**, 2192 (1969).
(19) S. Arnott and D. W. L. Hukins, *Biochem. Biophys. Res. Commun.*, **47**, 1504 (1972).
(20) F. H. C. Crick and A. Klug, *Nature (London)*, **255**, 530 (1975).
(21) In contrast to what is implied in ref 12 the dependence of τ on W (eq 1) is an *exact* result in the case of cyclopentane. The calculations of ref 10 have shown that eq 1 is the exact least energy path for cyclopentane.
(22) W. J. Adams, H. J. Geise, and L. S. Bartell, *J. Am. Chem. Soc.*, **92**, 5013 (1970).
(23) The conformations observed in crystals are equilibrium conformations that satisfy both the internal constraints of the molecule and the crystal packing requirements. In every crystal, the observed conformation lies at the minimum of the energy of the molecule plus that of the whole crystal lattice. For this reason, the observed conformation does not obey the Boltzmann distribution.
(24) M. Levitt, *Proc. Natl. Acad. Sci. U.S.A.*, **75**, 640 (1978).

Kinetics and Thermodynamics of the Reactions of Two Iron(III) Porphyrins with Imidazole and 1-Methylimidazole[1] in Dimethyl Sulfoxide

Robert F. Pasternack,* Bruce S. Gillies, and James R. Stahlbush

Contribution from the Department of Chemistry, Ithaca College, Ithaca, New York 14850. *Received September 15, 1977*

Abstract: The reactions of tetraphenylporphinatoiron(III) chloride and hemin chloride with imidazole and 1-methylimidazole have been studied in dimethyl sulfoxide at $\mu = 0.04$ M ($NaNO_3$). Stability constants have been determined for the reactions $SFeP + 2L \rightleftharpoons L_2FeP + S$ over a range of temperatures. There was no evidence for appreciable concentrations of LFeP in any of the systems studied. For $FeTPP^+$: $\Delta H^\circ = -10.7$ kcal/mol, $\Delta S^\circ = -13.8$ eu for imidazole and $\Delta H^\circ = -10.2$ kcal/mol, $\Delta S^\circ = -15.4$ eu for 1-methylimidazole. For hemin: $\Delta H^\circ = -8.0$ kcal/mol, $\Delta S^\circ = -4.6$ eu for imidazole and $\Delta H^\circ = -9.2$ kcal/mol, $\Delta S^\circ = -10.9$ eu for 1-methylimidazole. Although the thermodynamic parameters are quite similar for each of the metalloporphyrins with a given ligand, the kinetic features differ markedly. The hemin reactions are faster than those of $FeTPP^+$ and while $\tau^{-1} = k_f[L]^2 + k_r$ for $FeTPP^+$ with both ligands at all temperatures studied, for hemin the inverse relaxation time varies as $[L]^2$ at low concentrations of ligand only. At higher concentrations, the reaction approaches a first-order dependence on ligand. It is suggested that this more complicated kinetic profile for hemin reflects an alternative pathway to the formation of the diliganded adduct to the one applicable to the other iron(III) porphyrins thus far studied. For hemin, we suggest an activated complex in which the second ligand interacts with the iron atom *before* the spin state change has occurred.

The properties and reactivities of iron porphyrins are of considerable interest to chemists and biologists alike. The emphasis on iron porphyrins arises in part from the various roles these species play as prosthetic groups in the heme(Fe^{II})- and hemo(Fe^{III})proteins. Among the reactions displayed by these ubiquitous substances are oxygen binding for transport and storage as in the hemoglobins and myoglobins, electron transfer as in the cytochromes, and catalysis of peroxide decomposition (catalase) and activation (peroxidase). For several of these processes, the biological function of the metal porphyrin rests in part on its ability to exchange axial ligands. Thus many of the studies on model iron porphyrin systems have dealt with the thermodynamics and kinetics of axial ligand addition/substitution. However, mechanistic interpretations of previous studies of the kinetics of bonding of ligand molecules to iron(III) porphyrins have been obscured by complications such as mixed solvent media,[2] multiple forms of the attacking ligand and metalloporphyrin,[2,3] and the necessity of using micelles to solvate the porphyrin to prevent aggregation.[4] Even the NMR line broadening studies, which avoid the above difficulties, provide only a partial picture of axial ligation[5-11] since they yield information primarily on ligand dissociation kinetics.

The use of dimethyl sulfoxide as a solvent medium seems to effectively overcome many of the limitations of other investigations. A large number of iron porphyrins are soluble in this solvent; in the absence of added hydroxide there is little tendency for aggregation;[12] the aprotic nature of the solvent limits the number of metalloporphyrin and ligand forms which must be considered in discussing mechanistic pathways; the relatively high dielectric constant and donicity number of Me_2SO prevent extensive ion pairing in the medium and lead to solvent-coordinated metal sites;[13,14,15] and temperature-jump kinetic studies can be conveniently conducted using this solvent medium (cf. Figure 1). The reactions of iron(III) porphyrins with axial ligands are so rapid as to make the temperature-jump technique particularly useful for these investigations.

We are reporting on the thermodynamics and kinetics of the reactions of tetraphenylporphinatoiron(III) ($Fe^{III}TPP^+$) and hemin ($Fe^{III}PPIX^+$) with the ligands imidazole (Im) and 1-methylimidazole (1-CH_3Im) in a dimethyl sulfoxide medium. Both metalloporphyrins, in the absence of added nitrogenous bases, exist in solution as high-spin complexes in which the iron atom is significantly out of the plane defined by the pyrrole nitrogen atoms.[1,14,16] The coordination number of the iron

0002-7863/78/1500-2613$01.00/0